



Research Article

Impact of Organic Hydrocarbons on Fuel Properties and Engine Characteristics of Thermally Cracked Cashew Nut Shell Liquid

Gokul Raghavendra Srinivasan*, Aditya Mahajan, Rajiv Seth, Rakesh Mahajan

Research and Development Department, Steamax Envirocare India Private Limited, Janak Puri, Delhi-110058, India.

PAPER INFO

Paper History:

Received: 26 March 2022

Revised: 06 July 2022

Accepted: 07 July 2022

Keywords:

Cashew Nut Wastes,
Thermal Cracking,
Screw Press Extraction,
Anacardic Acid,
Cresol

ABSTRACT

The present study aims to explore the role of characterized hydrocarbons in thermally cracked shell liquid in determining its overall fuel properties and combustion characteristics in a CI engine. For this purpose, waste shell liquid was extracted from waste cashew nut shell by means of cold extraction technique using a simple electrically operated mechanical screw press, which reported maximum extractable oil content as 17.7 %. In addition, it was thermally cracked at 350-400 °C using conventional heating for both lab-scale and pilot-scale extraction. Based on its chemical composition, raw shell liquid contained anacardic acid and cardol, while thermally cracked shell liquid had cresol and methyl oleate as their dominant hydrocarbon compounds. Their composition was found to be 51.84 %, 33.68 %, 43.87 %, and 28.49 %, respectively. According to their contribution, both cyclic and aromatic as well as linear-chained hydrocarbons exhibited significant effect on the fuel properties of the cracked shell liquid, with carbon atoms contributing to its physical and thermal properties, whereas cyclic and aromatic hydrocarbons enhance its flow characteristics. Next, neat and blend samples of this cracked shell liquid with petrodiesel reported higher peak in-cylinder pressure by 5.6 % (on average) due to the presence of fatty acid esters, which induced early ignition and provided sufficient time for combustion. Meanwhile, higher emission levels were attributed by both cyclic and aromatic and linear-chained hydrocarbons, citing aromaticity and unsaturation in their molecules, which also resulted in reduced thermal efficiencies by 12.5 % (on average), upon accounting for their inferior calorific content. In conclusion, it is evident that hydrocarbons in these treated shell liquids play a significant role in their fuel properties and engine characteristics.

<https://doi.org/10.30501/jree.2022.335041.1349>

1. INTRODUCTION

Rise in environmental concerns and energy demand has increased the necessity to rely on renewable energy resources even for large-scale and industrial applications. These industrial applications include even food and food processing, which uses a large volume of biomass and helps reduce serious pollution threats and climate change issues [1]. One such biofuel is Cashew Nut Shell Liquid (CNSL) that enjoys a good potential in serving as an effective alternative fuel for supplying necessary energy [2].

To begin with, CNSL is a pericarp fluid of cashew nut, present inside the soft honey comb structure of its shell. Usually, it appears as a reddish brown liquid with high viscosity and is regarded as a cheap, yet effective, source for unsaturated phenols [3]. Although the thickness of these honey comb structures is about 1/8th of an inch, the availability/concentration of this CNSL-based oil content ranges between 30-35 wt % and varies from the nature of plant growth, cultivation technique, and geography [4].

Besides, this CNSL comprises 4 most dominant chemical compounds, namely anacardic acid, cardanol, cardol, and 2-methyl cardol and their distribution in the CNSL is entirely based on the extraction technique used for extracting this liquid from the shell [5]. By acknowledging this, variation of the distribution of these chemical compounds in the raw CNSL extracted by different rendering techniques is summarized in Table 1 and for different operating parameters in Table 2 [3, 6, 7]. In fact, numerous researchers reported the chemical composition and physicochemical properties of these CNSLs in addition to their extraction techniques in the past studies and considered them as the most predominantly found chemical compounds.

Drawing on the above findings, Kyei and Onyewuchi Akaranta (2019) studied the extraction technique and physicochemical properties of CNSL extracted from CNS upon synthesizing resin from these CNS-based liquids. Here, accelerated solvent extraction was identified as the most efficient technique and an average yield of 31 % of CNSL was reported. In terms of fuel properties, CNSL exhibited very high density (> 950 kg/m³) and acidity with slightly increased FFA content and very high saponification value (255.26 mg

*Corresponding Author's Email: gokusrinivasan@gmail.com (G.R. Srinivasan)
URL: https://www.jree.ir/article_155097.html

Please cite this article as: Srinivasan, G.R., Mahajan, A., Seth, R. and Mahajan, R., "Impact of organic hydrocarbons on fuel properties and engine characteristics of thermally cracked cashew nut shell liquid", *Journal of Renewable Energy and Environment (JREE)*, Vol. 10, No. 2, (2023), 81-94. (<https://doi.org/10.30501/jree.2022.335041.1349>).



KOH/g). Moreover, spectral analysis of extracted CNSL revealed its chemical nature as polymeric with a higher concentration of phenolic compounds [8].

Looking into the extraction techniques, Rodrigues et al. (2011) studied the effectiveness of different extraction methods in extracting CNSL and investigated their significance. Next, CNSLs extracted by roasting the waste cashew nut shells at slightly higher temperatures (180 and 200 °C) were considered as technical CNSL (T-CNSL) and were compared with the CNSL extracted at room temperature using screw press (CNSL-NP) and hexane-based solvent extraction

(CNSL-NS). Based on the characterization of chemical compounds, both CNSL-NP and -NS were reported to have a higher concentration of Anacardic acid and cardol and a lower concentration of cardanol than T-CNSL; however, natural extraction techniques were discriminated in terms of cardanol concentration variation. Besides, these naturally extracted liquids exhibited poor performance as a result of increased viscosity and impurity content and lower thermo-oxidative stabilities and ebullition temperature. Yet, CNSL extracted using cold solvent extraction retained their actual fuel properties as compared to other methods [9].

Table 1. Chemical composition (in %) of raw CNSLs extracted by various rendering techniques [3, 6]

Constituents	Pyrolysis	Decarboxylation	Soxhlet's extraction		SCW extraction	SC-CO ₂ extraction	Two-step extraction	
			Hexane	Methanol			Hexane-SCW	Methanol-SCW
Cardanol								
Saturated Cardanol			1.22	1.45	2.4	1.52	1.04	1.84
Monounsaturated Cardanol	54	65	26.64	27.19	68.93	1.09	48.84	49.22
Anacardic Acid								
Monounsaturated Anacardic Acid	5	2	27.9	19.06	9.47	52.24	18.64	11.4
Cardol								
Saturated Cardol	27	31	20.31	34.88	1.85	29.58	9.76	12.64
Monounsaturated Cardol	–	–	1.05	–	–	–	0.57	–
Di-unsaturated Cardol	–	–	7.62	10.39	–	6.72	4.13	6.07
Known Hydrocarbons								
Octacosene	–	–	–	–	4.91	–	2.25	2.04
Stigmasterol	–	–	–	–	3.44	–	1.57	1.43
Triacotene	–	–	3.33	3.41	–	4.31	1.85	5.45
β-Sitosterol	–	–	1.38	1.86	1.63	1.63	0.75	1.76
Unknown Hydrocarbons								
Hydrocarbon 1	–	–	5.7	–	–	–	–	3.33
Hydrocarbon 2	–	–	–	–	3.42	–	1.57	1.42
Hydrocarbon 3	–	–	–	–	3.29	–	1.51	1.37
Others	14	2	4.85	1.76	0.66	2.91	7.52	2.03

* SC: Supercritical; SCW: Supercritical Water; SC CO₂: Supercritical Carbondioxide

Table 2. Variation in chemical composition of CNSL with varying rendering techniques and operating parameters [3, 7]

Operating parameter (P bar/T °C)	SC-CNSL from CNS		SC-CNSL from CNS obtained through heat exchanger unit		SC-CNSL from Pyrolysis CNSL	
	Compound	Comp. %	Compound	Comp. %	Compound	Comp. %
200/60	Cardanol-C15	84.2	Cardanol	62.31	Cardanol diene	48.61
	Methyl Cardanol	2.83	Cardanol diene	31.24	2-methyl benzaldehyde	20.51
	Hexadecanoic acid	0.71	Heptadecane	0.77	3-ethyl phenol	7.64
	Cardanol-C13	0.69	8-methyl heptadecane	0.7	3-butyl phenol	1.39
	Oleic acid	0.62	Hexadecane	0.67		
			Pentadecane	0.67		
			2,6,10,14 tetra methyl pentadecane	0.65		
225/60	Cardanol-C15	86.26	Hexadecanoic acid	0.61	Cardanol diene	66.82
	Methyl Cardanol	3.11	Elicosane	0.47	Ethyloxybenzene	11.21
	Oleic acid	0.684			Acenaphthylene	7.12
	Cardanol-C13	0.65			3-ethyl phenol	3.31
	Hexadecanoic acid	0.56			3-butyl phenol	2.28
					Azulene	1.89

250/60	Cardanol-C15	64.89	Cardanol	81.54	Cardanol	64.91
	Diethyl Phthalate	12.34	2-methyl Cardanol diene	2.97	Propyl benzene	11.96
	Cardanol-C13	7.42	Tetradecanal	1.99	4-ethyl phenol	5.01
	Methyl Cardanol	3.03	Cardanol-C13	1.62	3-pentyl phenol	3.18
	Hexadecanoic acid	0.58	Hexadecanoic acid	1.27	Acenaphthylene	2.83
			Heptadecane	0.08	3-butyl phenol	1.35
		Pentadecane	0.04			
300/60	Cardanol-C15	61.34	Cardanol diene	81.94	Cardanol	80.5
	Diethyl Phthalate	13.35	2-methyl Cardanol diene	2.97	2-methyl benzaldehyde	8.73
	Cardanol-C13	2.32	Hexadecanoic acid	1.01	2-ethyl phenol	4.89
	Cardanol-C17	2.06	Oleic acid	0.98		
	Hexadecanoic acid	0.8				
	Oleic acid	0.67				

On account of their industrial significance, these CNSLs are used as raw materials for manufacturing paints and varnishes, polyurethane-based polymers, friction linings, foundry chemicals, surfactants, epoxy resins, laminating, and rubber compounding resins; and they even include intermediates for chemical industry [10, 11]. Although CNSL has its significance across the diversified industrial domain, it cannot be used directly for manufacturing or production process as each end product uses this CNSL in their respective processed manner. For this purpose, these CNSL are treated using numerous chemical treatment techniques; and the most commonly preferred technique uses chemical reactions such as transfer hydrogenation reactions, isomerization reactions, metathesis reactions, carbonylation reactions, polymerization reactions, isomerizing metathesis reaction, and isomerizing carbonylation reactions [12].

Although these techniques make CNSL as a highly efficient raw material or even more a suitable candidate for industrial applications, it fails to be processed into an ideal fuel compatible with combustion-based applications. Hence, any CNSL must be cracked or degraded into its smallest stable molecular form, and this must be achieved easily with minimal resource utilization. As a result, thermal and chemical cracking techniques can be identified as effective measures for cracking the macro molecules into simple aromatic and linear hydrocarbons. Specifically, thermal cracking is widely preferred for processing these CNSLs on industrial and large scales. Supporting this, Velmurugan et al. (2014) cracked the raw CNSL by heating it at slightly higher temperatures (200-400 °C) [13].

Furthermore, Vedharaj et al. (2016) reported the catalyst-assisted thermal cracking of CNSL before being subjected to evaluation in a Compression Ignition (CI) engine. Accordingly, the raw CNSL was preheated at 200 °C using an electric heater, followed by heating at 400 °C inside the main reactor. The vapor of CNSL was condensed using a water cooled condenser before passing the condensed cracked CNSL into the storage tank. Finally, the utilization of zeolite catalyst enhanced the rate of cracking of CNSL and overall yield [14].

These processed CNSLs serve as effective supplements or alternatives for existing biodiesel and neat diesel and can be used for wide varieties of combustion-based applications. However, in order to understand its effectiveness as fuel, it must be evaluated for its combustion and emission characteristics. Accordingly, Velmurugan et al. (2014) studied the performance of Thermally Cracked CNSL (TC-CNSL) in CI using a single-cylinder, water-cooled, diesel Direct Injection (DI), Kirloskar AV-1 diesel engine and reported that its characteristics was slightly identical to neat diesel.

Accordingly, TC-CNSL reported reduced CO and HC mission and increased NO_x and CO₂ emission on account of its fuel bound oxygen content. On the other hand, TC-CNSL exhibited increased rate of fuel consumption, which resulted in lower thermal efficiency. Interestingly, TC-CNSL exhibited a prolonged ignition delay followed by a longer combustion duration due to its aromatic compounds [13].

Next, Loganathan et al. (2020) tested the TC-CNSL in a CI engine by blending it with neat diesel and enriched the combustion products with hydrogen, which was administered into the engine in order to reduce the HC and CO emissions. In order to achieve a stable emission level, Exhaust Gas Recirculation (EGR) technique was employed on the engine with the circulation administered at 10 % of exhaust gas, while the flow rate of hydrogen was maintained at 6 LPM. The test results reported a simultaneous rise in the thermal efficiency up to 36.5 % and a reduction in HC and CO emission concentrations by 20 % and 10 %, respectively, while running at full load. On the contrary, these supplementary enrichments increased the NO_x emission by 40 %; however, reduced it upon introducing 30 % of EGR. In short, this study recommended using supplementary enrichment techniques for improving the engine properties of both ordinary and thermally cracked CNSLs [15].

Although numerous pieces of relevant literature report the availability, chemical composition, fuel properties, and engine characteristics of these CNSLs, the results obtained from these studies vary accordingly with rendering and processing techniques used. Hence, it is highly recommended that the molecular effect of various chemical compounds available in these raw and processed shell liquids be investigated so as to determine the parameters mentioned earlier. However, no previous studies have been focused or reported in relevance to the molecular impact on fuel properties and engine characteristics of CNSLs, though being reported for biodiesel fuels [16]. Considering this as an abridged research gap and an attempt to understand the molecular contribution, this present study exclusively focused on the role of characterized hydrocarbons in thermally cracked CNSLs in determining its fuel properties and engine characteristics. To be specific, this study used thermally cracked CNSLs extracted from waste CNS using mechanical screw press at lower temperatures, characterized them using GC and FT-IR spectroscopy, evaluated them for their fuel properties based on IS standards, and assessed them for the engine properties in single-cylinder CI engine.

2. MATERIALS AND METHODOLOGY

2.1. Proximate composition of cashew nut shell

Waste Cashew Nut shells (CNSs) used in the study were procured from local cashew processing units and were stored in air-tight containers to avoid any contamination. To begin with, proximate analysis of waste cashew nut shells to estimate their fraction mass of moisture and fixed carbon content, volatile matter, and ash residues was carried out by following the standard analytical methods, ASTM D 3173-3175. The fraction of moisture content in these shells was determined using ASTM D 3173 method in a drying oven. Then, the fraction of volatile matter was estimated as per ASTM D 3175 method, while the quantity of residual ash content was determined according to ASTM D 3174 method. Furthermore, the fixed carbon content in these shells was calculated by difference, accounting for the other calculated proximate compositions. Finally, the higher heating value of the waste shells was determined using a bomb calorimeter following the ASTM E 711 method, wherein the combustion was carried out in an environment with high pressure of oxygen (to ensure complete combustion) saturated with steam of water (to ensure that the whole water was converted into its liquid form).

2.2. Extraction of CNSL using mechanical extraction

Both lab-scale and Pilot-scale extraction of CNSL from CNS was executed by means of mechanical extraction method using a customized mechanical screw press. Here, the screw press was comprised of tapered compression screws mounted inside a cylindrical casing and was operated using an electric motor. The CNSs were fed into cylindrical casing using a feeding hopper attached transversely, and they were fed in the batch process. Furthermore, the compression screw was operated at a spindle speed of 7-13 rpm, while the maximum feeding and extraction rate were found to be 54-95 kg/hr and 11.93-14.90 kg/hr, respectively [17, 18]. It may be noted that

the waste CNS residues were re-fed into the screw press to extract the leftover CNSL from it.

2.3. Thermal cracking of CNSL

The extracted CNSL was thermally cracked using the high-temperature distillation technique on both lab and pilot scales. Accordingly, a simple distillation setup was used for cracking CNSL on a lab scale and it comprised a 500 mL flat bottomed flask mounted on a tripod stand and was fitted with a water jacketed condenser to cool the vapor collected post cracking. Here, a simple LPG fuelled gas burner was used for the purpose of heating and the temperature was maintained at 350-400 °C. In case of pilot-scale extraction, a stainless steel container was mounted on a customized LPG fuelled gas stove, which was used as the prime source for heating the CNSL inside it and was fitted to a water cooling jacket. The gas stove was capable of producing heat up to 550 °C, while the temperature was maintained at 410 °C throughout the cracking process. In the case of both of these setups, the condensates (TC-CNSL) were collected in the storage tanks and used for further analytical purposes.

2.4. Characterization of raw oil and TC CNSL

Both raw oil and TC CNSL were characterized for their chemical compounds using GC-MS and evaluation of function group using FT-IR spectroscopy, respectively. Tables 3 and 4 summarize the technical specifications of GC-MS and FT-IR spectroscopy [19, 20]. All the samples were prepared as per the standard sample preparation technique and obtained results were compared with those in standard library search databases to identify the suitable component and their activities.

Table 3. Technical specifications of gas chromatograph – mass spectrometer [19, 20]

Gas chromatograph		Mass spectrometer	
Equipment	Agilent 6890 chromatograph	Equipment	JOEL GC mate II bench top
Injector liner	direct/2 mm	Type	Double focusing magnetic sector MS
Column	15 m all tech ec-5 (25 µm ID, 0.25 µm thickness)	Operation mode	Electron ionization (EI) mode
Split ratio	10:01	Software	TSS-2001
Oven temperature	35 °C/2 min	Resolving power	1000 (20 % height definition)
Ramp	20 °C/min @ 300 °C for 5 min	Scanning feature	25 m/z to 700 m/z @ 0.3 s/scan
Helium carrier gas	2 ml/min (constant flow mode)	Inter scan delay	0.2 s

Table 4. Technical specifications of FT-IR spectrometer

JASCO	FTIR-4700
Standard wavenumber measurement range	7800 to 350 cm ⁻¹
Wavenumber range	15,000 to 0 cm ⁻¹
Detector	deuterated L-alanine doped triglycene sulphate-attenuated total reflectance (DLATGS.ATR)
Crystals	Zinc selenide (ZnSe)
Optical system	Single beam

2.5. Fuel properties evaluation for raw oil and TC CNSL

The necessary fuel properties and other physicochemical parameters were evaluated for both raw oil and TC CNSL as per Indian standards (IS: 1448). Accordingly, properties like density and kinematic viscosity were evaluated as per IS

standards using relative density balance method (IS:1448(P-32) 1992) and viscometer (IS:1448(P-25) 1976), respectively. Then, properties like flash and fire, ignition point, pour point, and calorific value were evaluated as per IS:1448(P-69) 2013 (Cleveland Open Cup Method), IS:1448(P-10/Sec-2) 2013, and IS:1448(P-6) 1984 (Bomb Calorimeter Method) testing

methods, respectively. Next, IS:1448(P-15) 2004 was followed to study the corrosiveness induced by the test samples on a copper strip, while the carbon residue content in these samples was evaluated using Conradson method as per IS:1448(P-122) 2013 testing standard.

2.6. Assessment of engine characteristics of TC-CNSL

Effects of identified hydrocarbons on combustion and emission characteristics of TC-CNSL were studied from their engine data and reported based on their testing in a single-cylinder CI engine, whose technical specifications are tabulated in Table 5 [16, 19]. For this purpose, three different samples of TC-CNSL, namely (i) TC-CNSL 20 blend, (ii) TC-CNSL 50 blend, and (iii) neat TC-CNSL or TC-CNSL 100 blend were prepared by blending with neat diesel in varying

proportions, in addition to comparing it as the reference sample. Here, TC-CNSL 20 sample represented the cracked biofuel at their minimal blending ratios and was considered as the globally accepted high-performance blend for any biofuel with neat diesel on global and commercial scales, whereas the TC-CNSL 50 sample signified the equivalent contribution of both cracked CNSLs and neat diesel. Moreover, the parameters studied from the engine characteristics include the peak pressure recorded, total delay period taken by fuel to initiate its combustion, rate of fuel consumed for unit power and their convertible efficiency, harmful emission gases like carbon monoxide (CO) and unburnt hydrocarbon (HC), and completely combusted carbon dioxide (CO₂) and nitrogen oxide (NO_x) emission.

Table 5. Technical specifications of Kirloskar TV1 Engine and AVL DI GAS 444 N Flue gas analyzer [19]

Kirloskar engine TV 1 specifications		AVL DI GAS 444 N (five gas analyzer)	
Type: Four-Stroke, Single-Cylinder Water Cooled		Measurement	Resolution
Rated power	5.2 KW	CO [0-15 Vol. %]	0.0001 Vol. %
Rated speed	1500 rpm	HC [0-20000 ppm Vol.]	1 ppm/10 ppm
Bore diameter (D)	87.5 mm	CO ₂ [0-20 Vol. %]	0.1 Vol. %
Stroke (L)	110 mm	O ₂ [0-25 Vol. %]	0.01 Vol. %
Compression ratio	17.5:1	NO _x [0-6000 ppm Vol.]	1 ppm Vol.

2.7. Error analysis

To ensure increased accuracy of the results, all the experiments were carried out in triplicates and results were reported in the form of mean \pm standard deviation. This deviation was taken into account as the variation results from the mean value and can be originated from different means, including human error and instrumental error. Equation 1 was used to calculate the standard deviation of each measured entity, where σ is the deviation from the mean value, x_i is the reported result, μ is the average mean of the reported results, and N is the number of times experiments were repeated ($N=3$, in this case) [20].

$$\sigma = \sqrt{\frac{\sum(x_i - \mu)^2}{N}} \quad (1)$$

3. RESULTS AND DISCUSSION

3.1. Proximate analysis of CNS

From the results of proximate analysis on cashew nut shell, it was clearly evident that the collected wastes were highly suitable for gasification. Table 6 summarizes the proximate composition of waste CNS estimated as per ASTM standards. It was observed that the average moisture content of cashew nut shell waste was 5.9 % and was well within the acceptable limit (below 15 %), as prescribed for any fuel [21], and this ensured its free flow and ability to produce good quality gas. Next, the average volatile matter content in cashew nut shell was estimated to be 74.83 %, and the higher amount of volatile matter was encouraged for its gasification. Then, the analysis of the suggested their average ash content at 0.9 % points to its suitability for gasification with minimum blocking of flow of air and fuel and formation of clinkers. Moreover, as the most desirable component for stating the volume of non-volatile carbon in the biomass, the average fixed carbon content in these waste shellst was calculated as 18.4 %.

Again, heating value of the biomass also decides its suitability for their gasification and the results present the average higher heating value of these cashew nut shells as 5036.8 Kcal/m³ (21.09 MJ/kg).

Table 6. Proximate composition of waste CNS

Proximate composition	CNS	Standard
Moisture (%)	5.9	ASTM D 3173
Volatile matter (%)	74.83	ASTM D 3175
Ash content (%)	0.9	ASTM D 3174
Fixed carbon (%)	18.4	By difference
Higher heating value (MJ/kg)	21.09	ASTM E 711

3.2. Extraction of raw CNSL

CNS, in this present study, had a maximum pericarp liquid (lipid) content of 23.8 % and this liquid played a significant role in protecting the seed kernel from harmful pests and moisture content entering into it [22, 23]. In general, maximum renderable oil content was found to be between 21.5 % and 22.9 %; however, extraction of CNSL using mechanical screw press yielded only up to 17.7 %. The reduction of oil content resulted from the lack of chemical interaction, wastage, and evaporation of highly volatile chemical compounds due to high compression force exerted by the mechanical components in the screw press. Eventually, slightly increased rendering yield was explained by the re-feeding of CNS residues into the press, which helped extract the leftover CNSL (upto 5.7 %) from the waste residues. Moreover, CNSL obtained by this method was highly viscous with increased concentration of impurities (CNSL purity: 83.2 wt %), in addition to lower boiling temperature and poor thermal oxidation stability [9].

3.3. GC and FT-IR characterization of raw CNSL

3.3.1. GC characterization

Based on the previous pieces of the literature, raw CNSL reportedly had 7-42 % cardol, 47-63 % anacardic acid, and 3-25 % Cardanol [5, 9]. From the present study, the chemical composition of raw CNSL was found to be anacardic acid (51.84 ± 1.14 %), cardol (33.68 ± 0.86 %), cardanol (8.11 ± 1.07 %), methyl cardol (0.35 ± 0.074 %), and others (6.02 ± 0.87 %), and it was in closer agreement with the chemical composition reported by the literature works mentioned earlier, in which CNSL was extracted through mechanical extraction. In fact, the reported chemical composition was widely different and irregular with respect to the chemical

composition of the raw CNSL extracted using other techniques. A significant change in GC composition was reported exclusively between anacardic acid and cardanol; the mentioned variation was dependent on the extraction technique. In this study, the higher composition of anacardic acid was reported as a result of cold extraction of CNSL. Table 7 consolidates the chemical compounds characterized in the raw CNSL using GC, and Figure 1 depicts the GC spectra of raw CNSL. In addition, Figures 2-4 illustrate the optimized 3D molecular structure of anacardic acid, cardol, and cardanol designed using Avogadro tool.

Table 7. Chemical compounds characterized in the raw CNSL using GC

Chemical compound	Oliveira et al., 2011 (in %)	TC-CNSL (present study) (in %)	Rodrigues et al., 2011 (in %)
Anacardic Acid	62.94	51.84	47
Cardol	6.99	33.68	42
Cardanol	24.52	8.11	3
2-Methylcardol	0.59	0.35	N.A.
Others	4.96	6.02	8

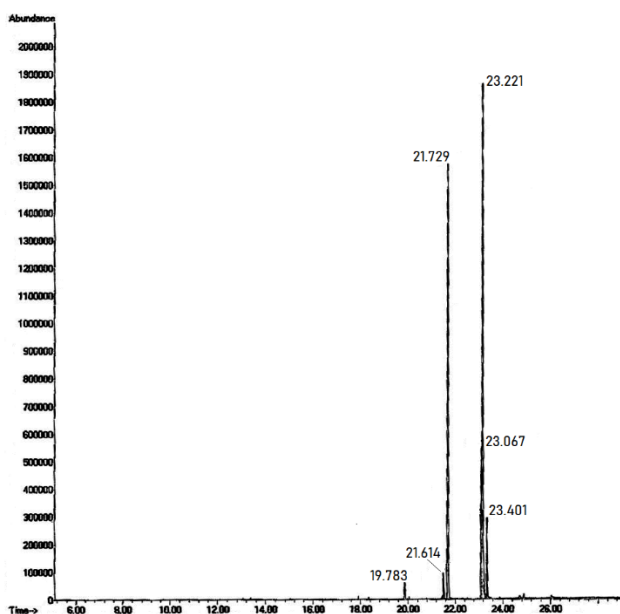


Figure 1. GC spectra of raw CNSL

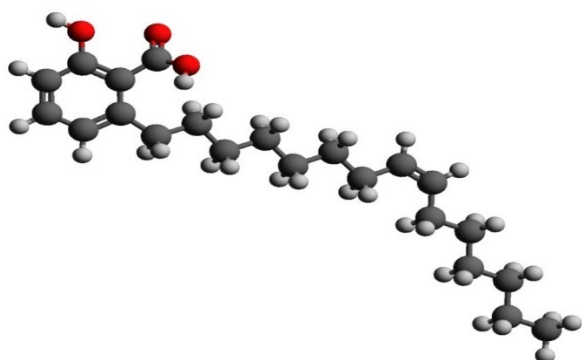


Figure 2. Optimized 3D molecular structure of anacardic acid developed using Avogadro tool (molecular formula: $C_{22}H_{34}O_3$; molecular weight: 346.5 g/mol)

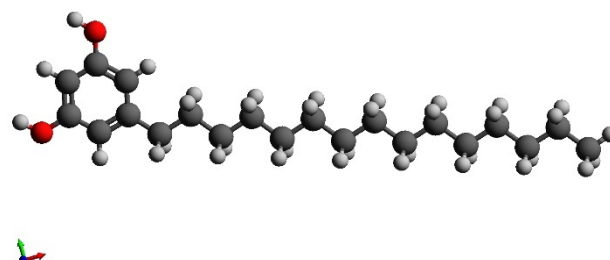


Figure 3. Optimized 3D molecular structure of cardol developed using Avogadro tool (molecular formula: $C_{21}H_{36}O_2$; molecular weight: 320.5 g/mol)

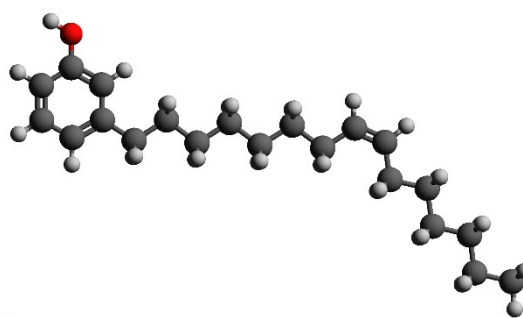


Figure 4. Optimized 3D molecular structure of cardanol developed using Avogadro tool (molecular formula: $C_{21}H_{34}O$; molecular weight: 302.5 g/mol)

3.3.2. FT-IR characterization

Table 8 consolidates the dominant peaks in the FT-IR spectra and chemical compounds contributing to these based on their corresponding bond activities in raw CNSL. First off, a broad peak at 3348.19 cm^{-1} reported the hydroxyl ($-OH$) stretching noted in polymeric compounds and was contributed by $-OH$ in cardol and cardanol. Then, another notable peak at 3074

cm^{-1} , related to the stretching of carbon and hydrogen, was found only in the aromatic compounds (anacardic acid, cardol, and cardanol). Likewise, peaks corresponding to unsaturation in hydrocarbon moieties of anacardic acid, cardol, and cardanol were reported at 3016 cm^{-1} . In addition, the asymmetric and symmetric stretching of alkyl C-H bond was considered based on the peaks reported at 2912 and 2859 cm^{-1} , respectively. The stretching of unsaturated carbon bonds ($\text{C}=\text{C}$) in the aromatic rings of anacardic acid, cardol, and cardanol were noted at two distinct peaks reported at 1637 cm^{-1} . Peak at 1444 cm^{-1} represented the C-H bending between the phenolic ring and hydrocarbon chain in the characterized

compounds. Meanwhile, the peak at 1373.4 cm^{-1} signified the O-H bending corresponding to the -OH bonded with aromatic rings of cardol and cardanol. Next, the peaks at 988 and 907 cm^{-1} corresponded to the $\text{C}=\text{C}$ bending in the polycardanol structure, which were reported at the conjugated *cis-trans* double bond and the terminal vinyl group. Moreover, the peak at 687 cm^{-1} corresponded to the $\text{C}=\text{C}$ bending of the vinyl group which is formed as the polyaromatic structure. Summing up, it was clearly evident that CNSL existed in polymeric form, with carboxylic and hydroxyl groups bonding to aromatic (phenolic) compounds. The same finding was achieved in the existing literature [24-26].

Table 8. Peaks and chemical compounds contributing to various bond activities in raw CNSL

Peak (cm^{-1})	Bond activity	Contributing chemical compound
3348.19	O-H stretching	Anacardic acid; cardol; cardanol
3074	Aromatic C-H stretching	Anacardic acid; cardol; cardanol
3016	Vinylic C-H stretching	Double bonds in hydrocarbons and aromatic rings
2912	Asymmetric C-H stretching	Alkyl groups in hydrocarbon chains
2859	Symmetric C-H stretching	Alkyl groups in hydrocarbon chains
1637	Aromatic $\text{C}=\text{C}$ stretching	Anacardic acid; cardol; cardanol
1444	Methyl group C-H bending	Anacardic acid; cardol; cardanol
1373.4	O-H bending	Anacardic acid; cardol; cardanol
1291.7	Ester group C-O stretching	Anacardic acid
988 and 907	$\text{C}=\text{C}$ bending (vinyl group)	Polyaromatic structure
687	$\text{C}=\text{C}$ bending (vinyl group)	Polyaromatic structure

3.4. Properties of raw CNSL bio oil

Based on the characterization data, CNSL is distributed at a higher concentration of anacardic acid and cardol followed by cardanol and it comprises aromatic hydrocarbons attached to long aliphatic carbon chains ranging up to 18 carbon atoms [27]. Owing to these aromatic rings and long carbon chains, raw CNSL displayed higher density and kinematic viscosity, which were 15.8% and $73.45 \text{ mm}^2/\text{s}$ higher than the permissible range for neat diesel, respectively [28]. Furthermore, increased molecular integrity in view of these phenolic ring structures provided the lowest pour point for CNSL ($-21 \text{ }^\circ\text{C}$) and ensured its functioning even at very low temperatures and in cold weather conditions. In addition, these anacardic acid and cardol contributed to the higher flash point

for CNSL, which made it safe for handling and transportation, besides increasing its auto ignition temperature slightly higher than neat diesel. The higher acidic pH value (4.1) for CNSL was accounted by the higher concentration of anacardic acid (51.84%), which was the result of controlled low-temperature extraction of CNSL. Upon investigating the proximate elemental composition, raw CNSL exhibited high carbon content of 81.02% , hydrogen content by 8.5% , and oxygen content by 8.6% . Besides, raw CNSL reported mild traces of nitrogen and sulphur content, which reduced its overall caloric value compared to its counter petro products. Table 9 summarizes the fuel properties of the raw CNSL evaluated as per IS and ASTM standards.

Table 9. Fuel properties of raw CNSL evaluated as per IS and ASTM standards

Parameters	Raw CNSL	Standards
Gross calorific value, kcal/kg	9061 ± 17	IS:1448(P-6) 1984
Kinematic viscosity @ $40 \text{ }^\circ\text{C}$, cSt	77.05 ± 1.14	IS:1448(P-25) 1976
Density @ $15 \text{ }^\circ\text{C}$, g/ml	0.9611 ± 0.01	IS:1448(P-32) 1992
Ash content, % by mass	1.3 ± 0.2	IS:1448(P-4) 1984
Flash point, $^\circ\text{C}$	206 ± 5	IS:1448(P-69) 2013
Pour point, $^\circ\text{C}$	-21 ± 2	IS:1448(P-10/Sec-2) 2013
Carbon residue (CCR), % by mass	6.45 ± 0.45	IS:1448(P-122) 2013
pH value	4.1 ± 0.4	By pH meter
Copper strip corrosion at $100 \text{ }^\circ\text{C}$ for 3 hours	1 No.	IS:1448(P-15) 2004
Ignition temperature, $^\circ\text{C}$	230 ± 8	IS:1448(P-69) 2013
Ultimate analysis		
Carbon, % by mass	81.02 ± 0.84	By CH analyzer

Hydrogen, % by mass	8.50 ± 0.12	By CH analyzer
Nitrogen, % by mass	0.30 ± 0.015	ASTM D3228
Sulphur, % by mass	0.09 ± 0.001	IS:1448(P-33) 1991
Ash, % by mass	1.31 ± 0.1	IS:1448(P-4) 1984
Moisture, % by mass	0.16 ± 0.03	ASTM D 6304
Oxygen, % by mass	8.62 ± 0.67	By difference

3.5. Thermally cracked CNSL (TC-CNSL)

3.5.1. GC characterization of TC-CNSL

Based on GC characterization on TC-CNSL (Table 10), methyl phenol (cresol), methyl oleate, methyl tetradecenoate, isopropyl cyclohexanedione, and 1-butyl-2-ethyl cyclobutane were identified as the dominant chemical compounds present in the thermally cracked CNSL (TC-CNSL). Eventually, the formation of linear chained and aromatic ring-shaped hydrocarbons is altogether justified by the thermal cracking of polymeric macro molecules available in raw CNSL [29], which induced cracking of linear HC from the aromatic ring in their carboxylic functional group. Further, TC-CNSL reported

a significant concentration of FAEs (upto 31.49 %), which made it suitable for combustion-based applications; in particular, methyl oleate played a major role in exhibiting fuel properties slightly similar to biodiesel. Interestingly, thermal cracking of CNSL also resulted in the formation of octadecane, sulfurous acid up to a concentration of 3.48 % and was found to be a source of sulphur in the resulting product. Figure 5 illustrates the GC spectra of TC-CNSL, whereas Figures 6-8 illustrate the optimized 3D molecular structure of cresol, methyl oleate, and methyl tetradecenoate designed using Avogadro tool.

Table 10. Chemical compounds characterized in the TC-CNSL using GC

Chemical compound	Composition (in %)	Chemical formula	Linearity/aromaticity
Phenol, 2-methyl	43.87	C ₇ H ₈ O	Aromatic
8-Octadecenoic acid, methyl ester	28.49	C ₁₉ H ₃₆ O ₂	Linear
Methyl 9-tetradecenoate	7.63	C ₁₅ H ₂₈ O ₂	Linear
Octadecane, sulfurous acid	3.48	C ₁₈ H ₃₉ SO ₃	linear
Ethanone, 1-cyclopentyl-cyclopentane	1.34	C ₉ H ₁₄ O ₂	Aromatic
4-Isopropyl-1, 3-cyclohexanedione	7.12	C ₉ H ₁₄ O ₂	aromatic
Cyclobutane, 1-butyl-2-ethyl	6.89	C ₁₀ H ₂₀	Aromatic
1-Dodecene, cyclododecane	1.18	C ₂₄ H ₄₇	aromatic

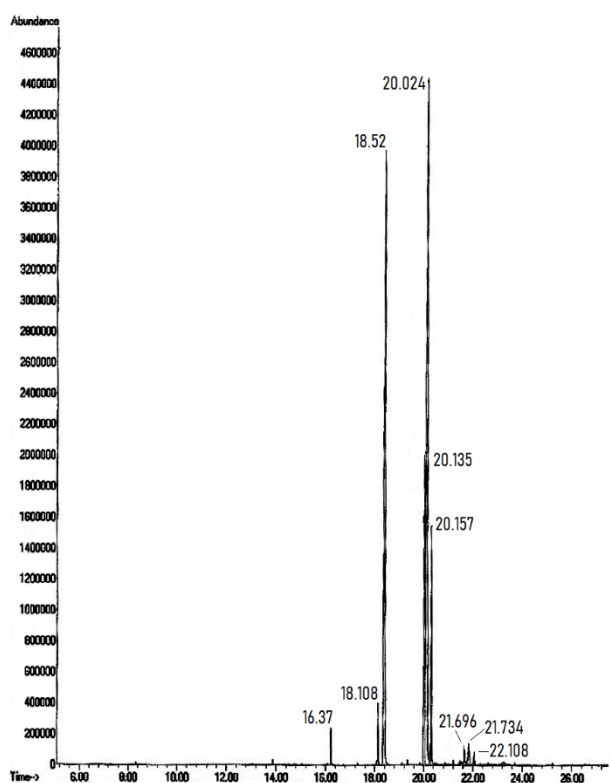


Figure 5. GC Spectra of TC-CNSL

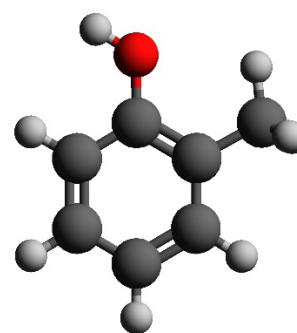


Figure 6. Optimized 3D molecular structure of cresol developed using Avogadro tool (molecular formula: C₇H₈O; molecular weight: 108.14 g/mol)

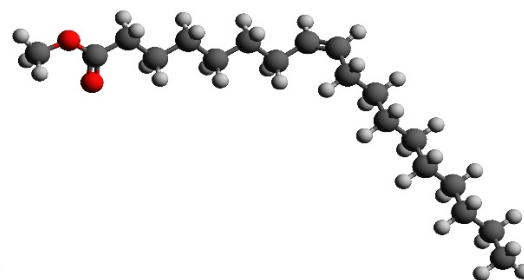


Figure 7. Optimized 3D molecular structure of methyl oleate developed using Avogadro tool (molecular formula: C₁₉H₃₆O₂; molecular weight: 296.5 g/mol)

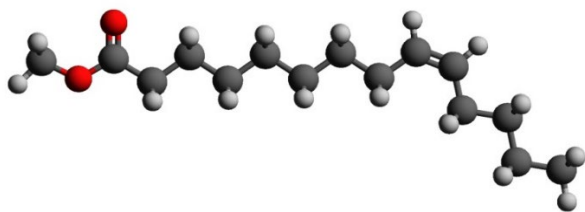


Figure 8. Optimized 3D molecular structure of methyl tetradecenoate developed using Avogadro tool (molecular formula: $C_{15}H_{28}O_2$; molecular weight: 240.4 g/mol)

3.5.2. FT-IR characterization of TC-CNSL

Based on the FT-IR spectral curve, a significant peak was reported at 3274 cm^{-1} , which signified the stretching of hydroxyl functional group (-OH) of methyl phenol (Cresol). Then, another peak between 2769 and 2934 cm^{-1} reported the asymmetric and symmetric stretching of C-H bonds in the alkyl chains of hydrocarbons. In the following, two significant

peaks at 1197 and 1738 cm^{-1} signified the presence of ester-based compounds (methyl oleate and methyl 9-tetradecenoate) [16] and played a significant role in improving the fuel properties of the resulting TC-CNSL and cresol. Moreover, another distinct peak at 1434 cm^{-1} signified the -OH bending and was related with the bending activities noted, exclusively, for any acidic compounds (cresol, octadecane, and sulphurous acid in this case). Furthermore, another distinct peak was reported at 1288 cm^{-1} , which corresponded to the stretching between carbon and oxygen molecule present in any aromatic esters. In addition, it contributed to the cyclic hydrocarbons available in it. Most importantly, the presence of octadecane and sulfurous acid was confirmed based on the peak reported at 1056 cm^{-1} , which was dedicated exclusively to the sulfoxide (S=O) stretching [30]. Table 11 consolidates the dominant peaks in the FT-IR spectra and chemical compounds contributing to these based on their corresponding bond activities in raw CNSL.

Table 11. Peaks and chemical compounds contributing to various bond activities in TC-CNSL

Peak (in cm^{-1})	Bond activity	Contributing chemical compound
3274	Phenols -OH stretching	Methyl phenol (Cresol)
1738	Ester C-O stretching	Methyl oleate, methyl 9-tetradecenoate
2769	Alkane C-H stretching	Hydrocarbon compounds
1434	Carboxylic (-OH) bending	Methyl phenol; octadecane, sulfurous acid
1288	Aromatic ester C-O stretching	Ethanone, 1-cyclopentyl-cyclopentane
1197	Ester C-O stretching	Methyl oleate, methyl 9-tetradecenoate
1056	Sulfoxide S=O stretching	Octadecane, sulfurous acid

3.6. Fuel Properties of TC-CNSL

According to the fuel properties of TC-CNSL, a drastic reduction in density and kinematic viscosity was reported and was estimated to be reduced by 8.75 % and 96 %, respectively, as compared to raw CNSL. Yet, higher density and viscosity than neat diesel (density: 830 kg/m^3 and kinematic viscosity: $2.47\text{ mm}^2/\text{s}$) were reported by 5.7 % and 21.5 %, respectively. Eventually, variation in density and kinematic viscosity was accounted for the formation of thermally cracked chemical compounds like cresol, FAEs, and cyclic hydrocarbons. In addition, the flash point of TC-CNSL was reduced by 46.6 % and was justified by the presence of FAEs in it, whereas its pour point was reduced by $24\text{ }^\circ\text{C}$ due to its aromatic and cyclic hydrocarbons, whose molecular

structure resembled the molecular structure of neat diesel. Furthermore, the formation of chemical compounds like cresol and Octadecane and sulfurous acid simply increased the pH by 43.2 % than compared to raw CNSL. Besides, high gross calorific value of TC-CNSL was explained by the presence of hydrocarbons, including long carbon chained molecules and combustible sulphur content; however, mild traces of nitrogen and sulphur content produced a slightly lower calorific value than neat diesel. The proximate elemental composition of TC-CNSL reported high carbon content of 84.16 %, hydrogen content of 11.45 %, and oxygen content of 4.01 %. Table 12 summarizes the fuel properties of TC-CNSL evaluated as per IS and ASTM standards.

Table 12. Fuel properties of TC-CNSL evaluated as per IS and ASTM standards

Parameters	TC-CNSL	Standards
Kinematic viscosity @ $40\text{ }^\circ\text{C}$, cSt	3.0 ± 0.62	IS:1448 (Pt-25) 2013, RA-2018
Gross calorific value, kcal/kg	10530 ± 23	IS:1448(Pt-6)1984, RA-2018
Density @ $15\text{ }^\circ\text{C}$, g/ml	0.877 ± 0.01	IS:1448 (Pt-32) 2019
Flash point (Abel), $^\circ\text{C}$	110 ± 5	IS:1448 (Pt-20) 2019
Copper strip corrosion at $100\text{ }^\circ\text{C}$ for 3 hours	1a	IS:1448 (Pt-15) 2004, RA-2016
Pour point, $^\circ\text{C}$	-45 ± 2.5	IS:1448 (Pt-10/Sec-2) 2013, RA-2018
pH	5.9 ± 0.6	By pH meter
Ultimate analysis, % by mass (IS:1448 (Pt-4) 1974, RA-2012)		
Ash content	0.001	IS:1448 (Pt-4) 1974, RA-2017
Carbon content	84.16 ± 0.75	ASTM D 5373-14, Guidelines
Hydrogen content	11.45 ± 0.5	ASTM D 5373-14, Guidelines

Nitrogen content	0.33 ± 0.025	ASTM D 5373-14, Guidelines
Sulphur content	0.05 ± 0.001	ASTM D 4239-17, (method B), guidelines
Oxygen content	4.01 ± 0.72	By calculation
Moisture (water) content, % by mass	Less than 0.05	IS:1448 (Pt-40) 2015

3.7. Combustion analysis

The stoichiometric air-to-fuel ratio required for combusting the TC-CNSL was calculated from the quantity of air needed for completely combusting its one mol. For this purpose, the quantity of air (N_{air}) was calculated using Equation 2, with numbers of carbon (N_C), hydrogen (N_H), and oxygen (N_O) molecules determined using the molecular formula of TC-CNSL, which was found to be $C_{12}H_{21}O$ [19]. As can be seen in this formulated molecular formula, the volume of air required for combusting one mol of TC-CNSL was calculated as 16.75 mols and the stoichiometric air-fuel ratio was 12.74:1. However, an excess amount of air is always needed to completely combust these TC-CNSLs; hence, the actual stoichiometric air to fuel ratio was adjusted to 19.12:1; thus, extra requirement for air was 1.5 times the calculated amount [31].

$$N_{AIR} = \frac{4N_C + N_H - 2N_O}{4} \quad (2)$$

Table 13. Engine characteristics of neat diesel and variation of engine data for TC-CNSL blends

Parameters	Unit	Diesel	TC-CNSL 20	TC-CNSL 50	TC-CNSL 100
Peak in-cylinder pressure	Bar	56.7	2.01 % ↑	4.74 % ↑	10.15 % ↑
Ignition delay	°CA	11.8	10.17 % ↑	15.25 % ↑	27.12 % ↑
Specific fuel consumption	Kg/kW-hr	0.37	5.46 % ↑	12.82 % ↑	24.91 % ↑
Brake thermal efficiencies	%	27.8	5.33 % ↓	11.89 % ↓	20.40 % ↓
Carbon monoxide emission	%	0.06	48.33 % ↑	196.41 % ↑	361.59 % ↑
Carbon dioxide emission	%	5.09	19.72 % ↑	41.67 % ↑	97.96 % ↑
Nitrogen oxide emission	PPM	405.9	15.59 % ↑	45.92 % ↑	89.35 % ↑
Unburnt hydrocarbon emission	PPM	52.6	15.21 % ↑	37.45 % ↑	74.90 % ↑
Exhaust gas temperature	°C	198.8	7.34 % ↑	22.69 % ↑	50.50 % ↑

To begin with, TC-CNSL had higher cylinder pressure than neat diesel (Figure 9) and it increased along with the concentration. This finding is justified by the early start and prolonged durations of their complete combustion, attributed by their higher cetane number, and fuel bound oxygen content [33]. Here, the higher concentration of oxygen molecules in TC-CNSL samples, especially from cresol, methyl oleate, methyl 9-tetradecenoate and 4-isopropyl-1, 3-cyclohexanedione, ensured their early ignition upon injection, followed by administering a complete oxidation, which resulted in liberation of a large amount of heat and pressure inside the cylinder. Accordingly, ignition delay was reduced at 100 % for neat TC-CNSL sample, citing the increased availability of fuel bound oxygen content from the injected fuel mass, which also helped meet the energy demand. However, ID of TC-CNSL samples remained higher than the neat diesel throughout the experimental runs (Figure 10) and were caused by physical and chemical delay raised due to the linear FAEs, followed by cyclic and aromatic hydrocarbons [34]. As a result of prolonged combustion duration and availability of surplus oxygen content, these TC-CNSL samples underwent complete combustion and generated significant heat, which resulted in higher EGTs and NO_x emission than neat diesel (Figures 11 and 12). In particular,

3.8. Engine characteristics of TC-CNSL

As can be seen from their engine characteristics (from Table 13), both neat TC-CNSL (TC-CNSL 100) and TC-CNSL blend samples reported superior combustion characteristics and mixed emission characteristics, besides reporting slightly poor performance characteristics. In fact, the increased combustion behavior of the biofuel samples was justified by their enhanced cetane number, which prolonged the duration of their combustion, whilst fuel-bound oxygen content ensured their complete oxidation [16, 32]. On the other hand, mixed emission concentrations and poor fuel performance were measured based on their increased density and viscosity, cyclic structure, aromaticity, unsaturation, and inferior calorific value. Here, this aromaticity and cyclic structure were predominantly contributed by cresol and 4-Isopropyl-1,3-cyclohexanedione, respectively, while unsaturation was affected by both long linear carbon chained (8-Octadecenoic acid, methyl ester and methyl 9-tetradecenoate) and aromatic hydrocarbons.

the oxidation of long-chain hydrocarbons like FAEs and cyclic hydrocarbons liberated a large amount of heat, fairly enough for nitrogen in the intake air to react with oxygen molecules to recombine into nitrogen oxides (NO_x) [35]. Here, both EGT and NO_x emissions increased proportionally with increase in concentration of TC-CNSL in the blended samples.

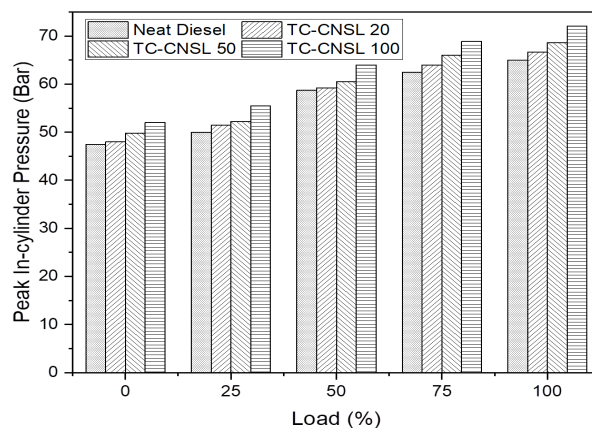


Figure 9. Peak in-cylinder pressure of neat diesel and TC-CNSL blends for varying engine loads

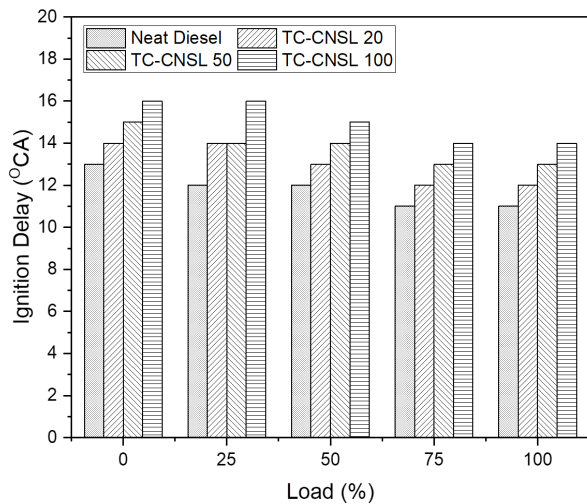


Figure 10. Ignition delay of neat diesel and TC-CNSL blends for varying engine loads

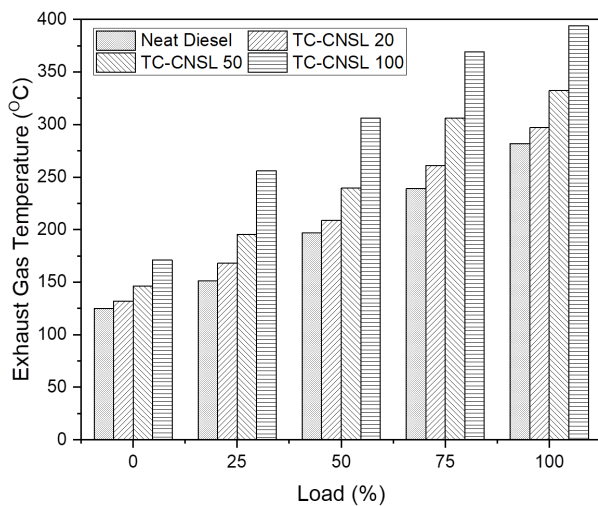


Figure 11. Exhaust gas temperature of neat diesel and TC-CNSL blends for varying engine loads

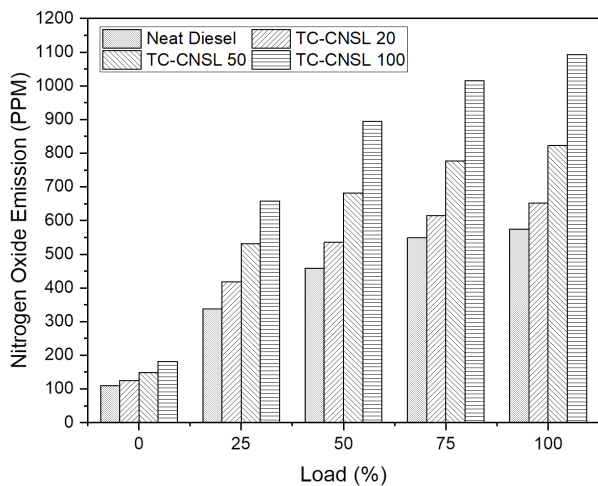


Figure 12. Nitrogen oxide emission of neat diesel and TC-CNSL blends for varying engine loads

In view of their complete oxidation, these TC-CNSL samples reportedly had a higher concentration of CO₂ emission than neat diesel (Figure 13) and remained higher for equivalent and neat TC-CNSL blend. This was accounted by

the fuel bound oxygen content from the hydrocarbons, which helped oxidize a large amount of hydrocarbon molecules in CO₂ and water, leaving behind a part of incomplete combustion and uncombusted by-products [36]. In this regard, carbon monoxide (CO) was produced as the incomplete by-product during the combustion and increased significantly with TC-CNSL concentration owing to their higher degree of unsaturated double bonds [19] (Figure 14). Unfortunately, these bonds failed to undergo complete combustion due to the need for high bond disassociation energy, which increased further at higher loads, citing the increased injection of fuel mass. On the other hand, from Figure 15, TC-CNSL samples reported a notable amount of unburnt hydrocarbon emission due to the lower adiabatic flame temperature near the wall surfaces and area surrounding large fuel droplets. Here, increased density and viscosity from both linear and cyclic hydrocarbons failed to atomize effectively, thus forming large droplets of fuel during injection and quenching the flame temperature inside the cylinder, thereby leaving behind a significant amount of unburnt hydrocarbon. Besides, unsaturation played a crucial role in contributing to this unburnt HC emission, as these unsaturated hydrocarbons needed more energy and heat for initiating combustion [31, 37].

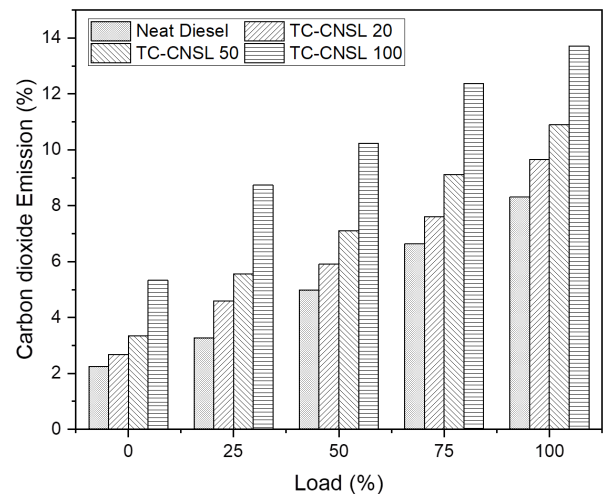


Figure 13. Carbon dioxide emission of neat diesel and TC-CNSL blends for varying engine loads

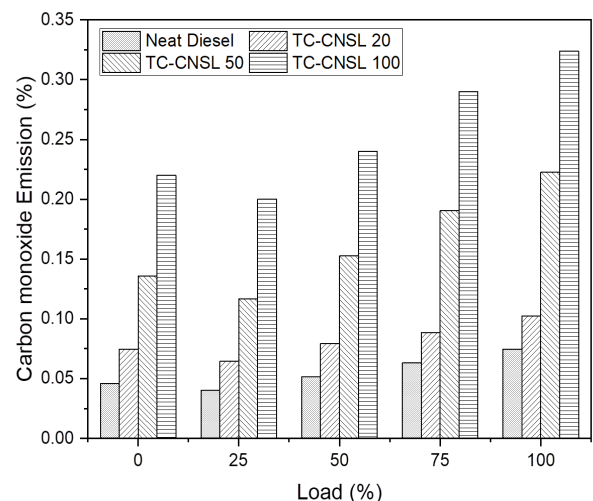


Figure 14. Carbon monoxide emission of neat diesel and TC-CNSL blends for varying engine loads

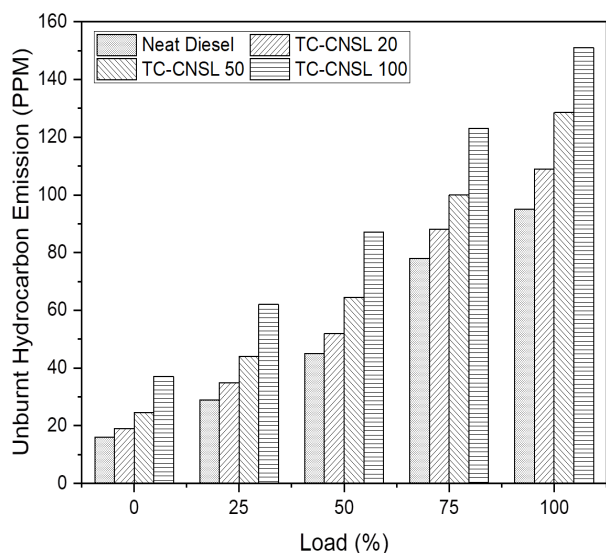


Figure 15. Unburnt hydrocarbon emission of neat diesel and TC-CNSL blends for varying engine loads

Based on their performance characteristics (Figures 16 and 17), TC-CNSL samples reportedly had a higher rate of fuel consumption and slightly reduced brake thermal efficiencies, citing their lower calorific content and higher density and viscosity than neat diesel. Here, the higher rates of density and viscosity for TC-CNSL samples were predominantly contributed by cresol, followed by FAEs and cyclic hydrocarbons, thus causing certain setbacks like increased quantity of injected fuel and poor atomization [16]. On the other hand, the absence of oxidizable molecules like nitrogen and small portion of sulphur content failed to report higher calorific value for TC-CNSL samples, thus requiring a greater amount of fuel for combustion to deliver equivalent energy as delivered by neat diesel [33, 38]. Moreover, their efficiency increased with engine load to maintain the engine speed all the time; however, it decreased with increasing TC-CNSL concentration, citing reduced calorific value due to the reduction of neat diesel concentration. Eventually, no knocking activities were reported for any test samples throughout the experimental runs; hence, this fuel is recommended given its compatibility with commercial applications.

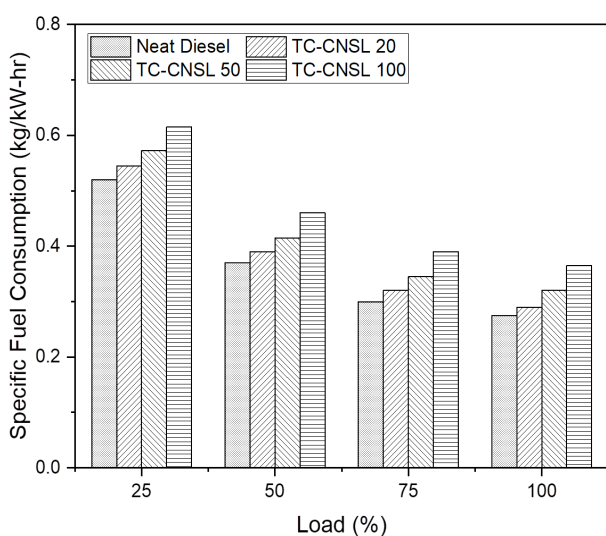


Figure 16. Specific fuel consumption of neat diesel and TC-CNSL blends for varying engine loads

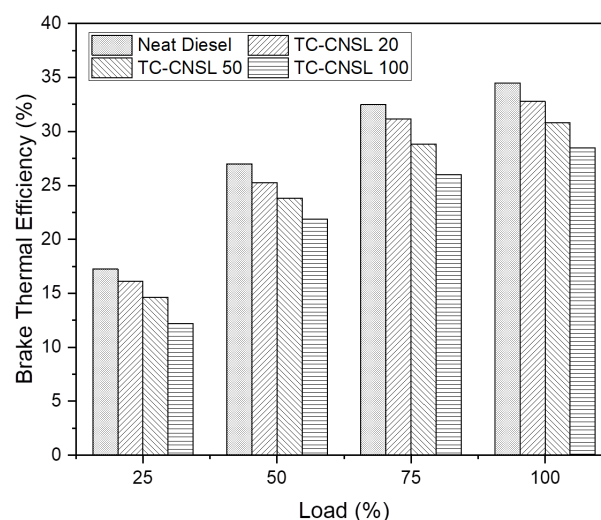


Figure 17. Brake thermal efficiencies of neat diesel and TC-CNSL blends for varying engine loads

4. CONCLUSIONS

Aimed at developing a suitable alternative to existing petrodiesel, this study achieved a sustainable biofuel from renewable biomass by thermally cracking the CNSL extracted from waste cashew nut shell by means of cold extraction technique. Effective utilization of this biofuel could be achieved upon evaluating its fuel properties and performance in CI engine, which in turn were determined by the chemical compounds available in it. Hence, it is of priority to understand the contribution of these chemical compounds on these entities. Thus, the impact of characterized hydrocarbons on deciding the overall fuel properties and engine characteristics of thermally cracked shell liquid was studied and the following were the major conclusions drawn from this study:

- (i) Both waste cashew nut shell and its liquid were identified as potential biomass feedstocks, which could be used as energy sources for both domestic and industrial purposes, accounting for their technical aspects.
- (ii) Waste CNS reported its maximum pericarp lipid content as 23.84 %; yet, the amount of CNSL rendered depends on the type of rendering technique. Next, the concentration of organic hydrocarbons in raw CNSL varied with respect to rendering technique; accordingly, the higher concentration of anacardic acid was reported in raw CNSL extracted using cold extraction technique.
- (iii) Thermal cracking of raw CNSL extracted using cold rendering was effective in the temperature range of 300-400 °C and it produced a higher concentration of cresol, methyl oleate, and tetradecenoate as the most dominant aromatic and linear chained hydrocarbons, respectively. It was also evident that thermal cracking of macromolecules was seen as an alternative means of synthesizing FAEs, besides transesterification.
- (iv) Fuel properties of TC-CNSL were deeply affected by the characterized hydrocarbons, with a large number of carbon atoms and long carbon chained molecules contributing to its physical and thermal properties, especially its calorific content. To be specific, cyclic and aromatic hydrocarbons facilitated enhancing their flow characteristics, whereas the presence of oxygen

molecules in the cracked shell liquid improved its cetane number.

- (v) Combustion of TC-CNSL in the CI engine presented a higher combustion rate and emission levels owing to the early start and prolonged duration of complete combustion contributed by both cyclic and aromatic and linear chained hydrocarbons including FAEs. Besides, aromaticity and unsaturation in these molecules increased their density and viscosity and reduced their calorific content, thereby resulting in reduced thermal efficiencies.

To sum up, it can be strongly concluded that the entire molecular composition of any CNSL is dependent on its rendering technique and thermal cracking of these liquids induces changes in their molecular structures, which has made a significant contribution to deciding its fuel properties and engine characteristics. Ultimately, understanding the impact of these molecules will facilitate (a) using this biofuel more effectively depending upon its end applications and (b) easily predicting its behavior during its life cycle, thereby ensuring sustainability and renewability throughout.

5. ACKNOWLEDGEMENT

Authors wish to thank the Management of Steamax Envirocare Private Limited for providing their support and facility to carry out this present work.

REFERENCES

- Sisco, M.R., Pianta, S., Weber, E.U. and Bosetti, V., "Global climate marches sharply raise attention to climate change: Analysis of climate search behavior in 46 countries", *Journal of Environmental Psychology*, Vol. 75, (2021), 101596. (<https://doi.org/10.1016/j.jenvp.2021.101596>).
- Lomonaco, D., Mele, G. and Mazzetto, S.E., "Cashew nutshell liquid (CNSL): From an agro-industrial waste to a sustainable alternative to petrochemical resources", *Cashew nut shell liquid*, Springer, Cham, (2017), 19-38. (https://doi.org/10.1007/978-3-319-47455-7_2).
- Taiwo, E.A., "Cashew nut shell oil—A renewable and reliable petrochemical feedstock", *Advances in Petrochemicals*, Vol. 1, (2015), 13. (<https://www.intechopen.com/chapters/48869>).
- Viswalingam, K. and Emerson Solomon, F., "A process for selective extraction of cardanol from Cashew Nut Shell Liquid (CNSL) and its useful applications", *International Journal of Scientific & Engineering Research*, Vol. 4, No. 3, (2013), 140-144. (<https://citeseerx.ist.psu.edu/document?repid=rep1&type=pdf&doi=1403141c531df86831c96b16626232c7641097fb>).
- Oliveira, M.S.C., de Moraes, S.M., Magalhães, D.V., Batista, W.P., Vieira, Í.G.P., Craveiro, A.A., de Maneses, J.E.S.A., Carvalho, A.F.U. and de Lima, G.P.G., "Antioxidant, larvicidal and anti acetylcholinesterase activities of cashew nut shell liquid constituents", *Acta Tropica*, Vol. 117, No. 3, (2011), 165-170. (<https://doi.org/10.1016/j.actatropica.2010.08.003>).
- Yuliana, M., Tran-Thi, N.Y. and Ju, Y.H., "Effect of extraction methods on characteristic and composition of Indonesian cashew nut shell liquid", *Industrial Crops and Products*, Vol. 35, No. 1, (2012), 230-236. (<https://doi.org/10.1016/j.indcrop.2011.07.007>).
- Patela, R.N., Bandyopadhyay, S. and Ganesh, A., "Selective extraction of cardanol and phenols from cashew nut shell liquid obtained through pyrolysis of cashew nut shells", *Proceedings of the Indian Chemical Engineering Congress, Novel Separation Processes Session (CHEMCON-2005)*, 14-17.
- Kyei, S.K. and Onyewuchi Akaranta, G.D., "Extraction, characterization, and application of cashew nut shell liquid from cashew nut shells", *Proceeding of China-Africa Urban Development Forum (CAUDF)*, University of Cape Coast, Cape Coast, Ghana, (2019), 104. (https://uilspace.unilorin.edu.ng/bitstream/handle/20.500.12484/7918/FINALCAUDF_2020_July_2020.pdf?sequence=1&isAllowed=y#page=113).
- Rodrigues, F.H., França, F.C., Souza, J.R., Ricardo, N.M. and Feitosa, J., "Comparison between physico-chemical properties of the technical Cashew Nut Shell Liquid (CNSL) and those natural extracted from solvent and pressing", *Polímeros*, Vol. 21, (2011), 156-160. (<https://doi.org/10.1590/S0104-14282011005000028>).
- Lubi, M.C. and Thachil, E.T., "Cashew Nut Shell Liquid (CNSL)-A versatile monomer for polymer synthesis", *Designed Monomers and Polymers*, Vol. 3, No. 2, (2000), 123-153. (<https://doi.org/10.1163/156855500300142834>).
- Sharma, P., Gaur, V.K., Sirohi, R., Larroche, C., Kim, S.H. and Pandey, A., "Valorization of cashew nut processing residues for industrial applications", *Industrial Crops and Products*, Vol. 152, (2020), 112550. (<https://doi.org/10.1016/j.indcrop.2020.112550>).
- Mubofu, E.B. and Mgaya, J.E., "Chemical valorization of cashew nut shell waste", *Topics in Current Chemistry*, Vol. 376, No. 2, (2018), 1-15. (<https://doi.org/10.1007/s41061-017-0177-9>).
- Velmurugan, A., Loganathan, M. and Gunasekaran, E.J., "Experimental investigations on combustion, performance and emission characteristics of thermal cracked cashew nut shell liquid (TC-CNSL)-diesel blends in a diesel engine", *Fuel*, Vol. 132, (2014), 236-245. (<https://doi.org/10.1016/j.fuel.2014.04.060>).
- Vedharaj, S., Vallinayagam, R., Yang, W.M., Saravanan, C.G. and Roberts, W.L., "Synthesis and utilization of catalytically cracked cashew nut shell liquid in a diesel engine", *Experimental Thermal and Fluid Science*, Vol. 70, (2016), 316-324. (<https://doi.org/10.1016/j.expthermflusci.2015.09.026>).
- Loganathan, M., Thanigaivelan, V., Madhavan, V.M., Anbarasu, A. and Velmurugan, A., "The synergetic effect between hydrogen addition and EGR on cashew nut shell liquid biofuel-diesel operated engine", *Fuel*, Vol. 266, (2020), 117004. (<https://doi.org/10.1016/j.fuel.2019.117004>).
- Srinivasan, G.R., Shankar, V., Chandra Sekharan, S., Munir, M., Balakrishnan, D., Mohanam, A. and Jambulingam, R., "Influence of fatty acid composition on process optimization and characteristics assessment of biodiesel produced from waste animal fat", *Energy Sources, Part A: Recovery, Utilization, and Environmental Effects*, (2020), 1-19. (<https://doi.org/10.1080/15567036.2020.1771477>).
- Garkal, D.J. and Bhande, R.S., "Review on extraction and isolation of cashew nut shell liquid", *International Journal of Innovations in Engineering Research and Technology*, Vol. 1, No. 1, (2014). (<https://repo.ijert.org/index.php/ijert/article/download/192/180/357>).
- Sivakumar, S., Venkatachalam, R., Nedunchezian, N., Sivakumar, P. and Rajendran, P., "Processing of cashew nut shell and feasibility of its oil as bio fuel in compression ignition engine", *Journal of Chemical and Pharmaceutical Sciences*, (Special Issue), Vol. 4, (2014), 133-135. (<https://jchps.com/specialissues/Special%20issue4/jchps%2047%20siva%20kumar%20s%20133-135.pdf>).
- Srinivasan, G.R., Shankar, V. and Jambulingam, R., "Experimental study on influence of dominant fatty acid esters in engine characteristics of waste beef tallow biodiesel", *Energy Exploration & Exploitation*, Vol. 37, No. 3, (2019), 1098-1124. (<https://doi.org/10.1177/0144598718821791>).
- Jambulingam, R., Srinivasan, G.R., Palani, S., Munir, M., Saeed, M. and Mohanam, A., "Process optimization of biodiesel production from waste beef tallow using ethanol as co-solvent", *SN Applied Sciences*, Vol. 2, No. 8, (2020), 1-18. (<https://doi.org/10.1007/s42452-020-03243-7>).
- Motta, I.L., Miranda, N.T., Maciel Filho, R. and Maciel, M.R.W., "Biomass gasification in fluidized beds: A review of biomass moisture content and operating pressure effects", *Renewable and Sustainable Energy Reviews*, Vol. 94, (2018), 998-1023. (<https://doi.org/10.1016/j.rser.2018.06.042>).
- Pandiyan, C.V., Shylaja, G., Srinivasan, G.R. and Saravanan, S., "Studies on use of Cashew Nut Shell Liquid (CNSL) in biopesticide and biofertilizer", *Nature Environment & Pollution Technology*, Vol. 19, No. 1, (2020), 103-111. ([https://neptjournal.com/upload-images/9\)B-3614.pdf](https://neptjournal.com/upload-images/9)B-3614.pdf)).
- Liu, W., Yue, Y., Tang, F., Qin, D., Hua, R. and Cao, H., "Fungicidal and insecticidal activities of CNSL", *Journal of Anhui Agricultural University*, Vol. 37, No. 4, (2010), 753-756.
- Achi, S.S. and Myina, O.M., "Preliminary investigation of Kaduna-Grown cashew nutshell liquid as a natural precursor for dyestuffs, pigments and binders for leather finishing", *Nigerian Journal of Chemical Research*, Vol. 16, (2011), 9-14. (https://www.researchgate.net/publication/281319361_Preliminary_Investigation_of_Kaduna-

- [Grown Cashew Nutshell Liquid as a Natural Precursor for Dyestuffs Pigments and Binders for Leather Finishing](#)).
25. Balgude, D. and Sabnis, A.S., "CNSL: An environment friendly alternative for the modern coating industry", *Journal of Coatings Technology and Research*, Vol. 11, No. 2, (2014), 169-183. (<https://doi.org/10.1007/s11998-013-9521-3>).
 26. Srivastava, R. and Srivastava, D., "Mechanical, chemical, and curing characteristics of cardanol–furfural-based novolac resin for application in green coatings", *Journal of Coatings Technology and Research*, Vol. 12, No. 2, (2015), 303-311. (<https://doi.org/10.1007/s11998-014-9630-7>).
 27. Morais, S.M., Silva, K.A., Araujo, H., Vieira, I.G., Alves, D.R., Fontenelle, R.O. and Silva, A., "Anacardic acid constituents from cashew nut shell liquid: NMR characterization and the effect of unsaturation on its biological activities", *Pharmaceuticals*, Vol. 10, No. 1, (2017), 31. (<https://doi.org/10.3390/ph10010031>).
 28. Ike, D.C., Ibezim-Ezeani, M.U. and Akaranta, O., "Cashew nutshell liquid and its derivatives in oil field applications: An update", *Green Chemistry Letters and Reviews*, Vol. 14, No. 4, (2021), 620-633. (<https://doi.org/10.1080/17518253.2021.1991485>).
 29. Lomonaco, D., Maia, F.J.N., Clemente, C.S., Mota, J.P.F., Junior, A.E.C. and Mazzetto, S.E., "Thermal studies of new biodiesel antioxidants synthesized from a natural occurring phenolic lipid", *Fuel*, Vol. 97, (2012), 552-559. (<https://doi.org/10.1016/j.fuel.2012.01.059>).
 30. Keating, C.S., McClure, B.A., Rack, J.J. and Rubtsov, I.V., "Sulfoxide stretching mode as a structural reporter via dual-frequency two-dimensional infrared spectroscopy", *The Journal of Chemical Physics*, Vol. 133, No. 14, (2010), 144513. (<https://doi.org/10.1063/1.3482708>).
 31. Raman, L.A., Deepanraj, B., Rajakumar, S. and Sivasubramanian, V., "Experimental investigation on performance, combustion and emission analysis of a direct injection diesel engine fuelled with rapeseed oil biodiesel", *Fuel*, Vol. 246, (2019), 69-74. (<https://doi.org/10.1016/j.fuel.2019.02.106>).
 32. Srinivasan, G.R., Palani, S., Munir, M., Saeed, M., Thangavelu, L., Mohanam, A. and Jambulingam, R., "Engine characteristics study on beef tallow biodiesel produced by ethanol based co-solvent transesterification", *Energy Sources, Part A: Recovery, Utilization, and Environmental Effects*, (2020), 1-21. (<https://doi.org/10.1080/15567036.2020.1826014>).
 33. Miron, L., Chiriac, R., Brabec, M. and Bădescu, V., "Ignition delay and its influence on the performance of a diesel engine operating with different diesel–biodiesel fuels", *Energy Reports*, Vol. 7, (2021), 5483-5494. (<https://doi.org/10.1016/j.egy.2021.08.123>).
 34. Brezinsky, K., "The high-temperature oxidation of aromatic hydrocarbons", *Progress in Energy and Combustion Science*, Vol. 12, No. 1, (1986), 1-24. ([https://doi.org/10.1016/0360-1285\(86\)90011-0](https://doi.org/10.1016/0360-1285(86)90011-0)).
 35. Talibi, M., Hellier, P. and Ladommatos, N., "Impact of increasing methyl branches in aromatic hydrocarbons on diesel engine combustion and emissions", *Fuel*, Vol. 216, (2018), 579-588. (<https://doi.org/10.1016/j.fuel.2017.12.045>).
 36. Siegl, W.O., McCabe, R.W., Chun, W., Kaiser, E.W., Perry, J., Henig, Y.I., Trinker, F.H. and Anderson, R.W., "Speciated hydrocarbon emissions from the combustion of single component fuels, I. Effect of fuel structure", *Journal of the Air & Waste Management Association*, Vol. 42, No. 7, (1992), 912-920. (<https://doi.org/10.1080/10473289.1992.10467041>).
 37. Jambulingam, R., Shankar, V., Palani, S. and Srinivasan, G.R., "Effect of dominant fatty acid esters on emission characteristics of waste animal fat biodiesel in CI engine", *Frontiers in Energy Research*, Vol. 7, (2019), 63. (<https://doi.org/10.3389/fenrg.2019.00063>).
 38. Hellier, P., Talibi, M., Eveleigh, A. and Ladommatos, N., "An overview of the effects of fuel molecular structure on the combustion and emissions characteristics of compression ignition engines", *Proceedings of the Institution of Mechanical Engineers, Part D: Journal of Automobile Engineering*, Vol. 232, No. 1, (2017), 90-105. (<https://doi.org/10.1177/0954407016687453>).